International Journal of Scientific Engineering and Research (IJSER)
ISSN (Online): 2347-3878
Index Copernicus Value (2015): 56.67 | Impact Factor (2017): 5.156

Modeling Plastic Fracture by Stillinger-Weber Potential-Embedded Discretized Virtual Internal Bond

Dina Kon Mushid

School of Naval Architecture, Ocean and Civil Engineering, Shanghai Jiao Tong University, Shanghai, 200240, China

Abstract: ***The failure of material always involves with the plastic deformation and fracturing process. For the plastic deformation, the continuum plastic mechanics can competently deal with the plastic deformation through a yield function and the flow rule. However, the continuum mechanics method has some limitations in dealing with the fracture problem due to that it cannot account for the microstructure of the material. The lattice model can simulate the fracture problem very well, but it is inadequate in dealing with plastic deformation. To unify the plasticity and the fracture together on the bond level, the present paper employed the Stillinger-Weber potential-based discretized virtual internal bond (SW-DVIB) method. DVIB is a kind of lattice model. It considers material to consist of bond cells. Each bond cell can take any geometry with any number of bonds. In original DVIB, the interaction between particles in a cell is characterised by an interatomical bond potential, which intrinsically contains the microfracture mechanism. However, because the interatomical potential only accounts for the effect of the bond stretch, the Poisson ratio it represents is fixed. To remedy this drawback, in the SW-DVIB the SW-potential is adopted to characterise the energy of a bond cell. Due to that, the SW-potential can simultaneously account for the bond angle and stretch effect; the SW-potential can represent the variable Poisson ratio. In this paper, the SW-DVIB is adopted to model the elastoplastic fracture. The plasticity is considered in the two-body potential. That is before the bond reaches its yielding point, this bond is linear elastic. After it reaches the yielding point, the bond enters the ideal plastic state. The irreversible deformation is reflected by following different loading-unloading paths. The bond does not rupture until its deformation reaches the limit value, which is related to the bond cell size and the macro fracture energy of the material. The three-body potential is kept linear elastic until the normal bond is ruptured. By this method, several examples were simulated. It is suggested that the irreversibility feature of the plastic deformation can be well captured. It can simulate the fracture propagation of material with the conservation of the fracture energy. The present paper provides an efficient approach to the elastoplastic fracture simulation.***

Keywords: plastic deformation, lattice model, plastic fracture, modified Stillinger- Weber potential, discretised virtual internal bond

1. Introduction

For the common engineering material, the fracture always goes together with the plastic deformation. How to consider the plastic deformation and fracture together has been an important topic since the plastic deformation takes a critical part in the fracturing process. The plastic deformation is usually localized before fracture, which cannot be ignored to understand the failure mechanism of materials. From a general viewpoint, continuum plasticity is a smooth irreversible deformation process, which is characterized by the yield surface and flow rules. The increment of the plastic strain tensor is described by the derivative of the flow potential with respect to the corresponding stress tensor. However, the continuum plasticity theory cannot be directly used to the lattice model. Xu et al [1] have ever combined the continuum plastic theory with the lattice model. In their method, the total strain is decomposed into the elastic and plastic part. For the elastic part, the micro lattice model is adopted while for the plastic part, the continuum plastic theory is adopted. Some other scholars considered the plastic deformation directly on the micro bond level. For instance, Zapperi et al [2], Seppala et al [3], Picallo et al [4] considered the plasticity in the arbitrary fuse grid which is analogous to the lattice structure. These progresses suggest that it is a feasible approach to reflect the plastic deformation on the micro bond level. More recently, Ding et al [5] accounted for the plastic deformation in the discretized virtual internal bond (DVIB) model introduced by Zhang [6]. DVIB [6] is a new lattice model which is different from the conventional one in that it can capture the meso structural characteristics of material composed of grains on mesoscale. Though the elastoplastic DVIB [5] can reproduce the plastic deformation to great extent, the Poisson ratio represented by this model is fixed. This is due to the two-body potential used in the DVIB, which misses the contribution of bond rotation. To overcome the limitation of Poisson ratio, Zhang and Chen [8] used the modified Stillinger–Weber (SW) potential to describe the total energy of a bond cell of DVIB. Here, term the SW potential-based DVIB as SW-DVIB. Because the SW potential can account for both the bond angle and the bond stretch effect, the SW-DVIB can represent the variable Poisson ratios. To extend the SW-DVIB to the plastic case in this paper, we embed the plastic deformation into the two-body interaction of the modified SW potential and keep the three-body interaction elastic. By this means, the SW-DVIB can account for the plastic deformation on one hand. On the other hand, it can represent the variable Poisson ratios.

2. Brief introduction to the SW-DVIB

The SW potential developed in [9], is a combination of two and three body interactions. It means that the bond energy is not only related to the bond length, but also related to the bond angles subtended to by the given bond and other bonds. Originally, the SW potential was specially used to simulate the silicon material since the reference bond angle is the

ideal tetrahedral angle. In 2014, the SW potential was modified by Zhang et al [8]. In the modified version of SW potential, the bond angle in the reference configuration, rather than the ideal tetrahedral angle, is taken as the reference bond angle value. Therefore, the modified SW-potential can be used to the material other than silicon. The SW potential takes:

$$\Phi = \sum_{i<j} \Phi_2\left(r_{ij}\right) + \sum_{\substack{i\neq j \\ j<k}} \Phi_3\left(r_{ij}, r_{ik}, \theta_{ijk}\right) \quad (1)$$

In which Φ_2, Φ_3 stands for the two- and three-body interaction, respectively; r_{ij} the bond length of bond vector $\mathbf{r}_{ij}$; θ_{jik} the bond angle subtended by the bond vector $\mathbf{r}_{ij}$, $\mathbf{r}_{ik}$ at vertex i, shown in Fig.1.

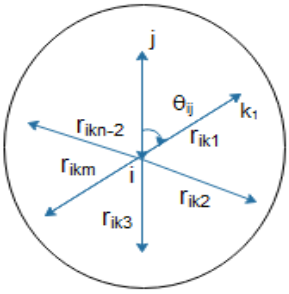

Figure 1: The conjugate bond vectors subtended at a given particle i in a discrete system with N particles.

In the modified SW potential shown in [8], the Φ_2, Φ_3 are respectively:

$$\Phi_2\left(\tilde{r}_I\right) = A\left(B\tilde{r}_I^{-p} - \tilde{r}_I^{-q}\right)\exp\left[\left(\tilde{r}_I - r_0^*\right)^{-1}\right]$$
$$\Phi_3\left(\tilde{r}_I, \tilde{r}_J, \theta_{IJ}\right) = \lambda\left(\cos\theta_{IJ} - \cos\theta_{IJ0}\right)^2 \exp\left[\gamma\left(\tilde{r}_I - r_0^*\right)^{-1} + \gamma\left(\tilde{r}_J - r_0^*\right)^{-1}\right] \quad (2)$$

In which $\tilde{r}_I$, $\tilde{r}_J$ are the normalized bond length, $\tilde{r}_I = r_{ij}/l_0, \tilde{r}_J = r_{ik}/l_0$; θ_{IJ0} stands for the bond angle subtended by the bond $\mathbf{r}_{ij}$ and $\mathbf{r}_{ik}$ in the reference configuration whereas θ_{IJ} its value in the current configuration.

The linear elastic SW-potential developed by Zhang et al. [7] reads:

$$\Phi_2 = \frac{1}{2} A l_0^2 \left(\tilde{r}_I - 1\right)^2 \quad (3.1)$$

$$\Phi_3 = \frac{1}{2} \lambda \left(\theta_{IJ} - \theta_{IJ0}\right)^2 \quad (3.2)$$

or the lattice bond cell shown in Fig.1, the total strain energy can be written as

$$W = \frac{1}{2}\sum_{I}^{N(N-1)} \Phi_2\left(\tilde{r}_I\right) + \frac{1}{2}\sum_{I}^{N(N-1)}\sum_{J}^{N-2} \Phi_3\left(\tilde{r}_I, \tilde{r}_J, \theta_{IJ}\right) \quad (4)$$

In which N denotes the total particle number in a unit cell with $\mathbf{r}_{ij} \neq \mathbf{r}_{ji}$.

By Eq.(5), the particle force vector $\mathbf{F}$ and the stiffness matrix $\mathbf{K}$ of this bond cell are respectively derived as

$$F_i = \frac{\partial W}{\partial u_i} \quad (5)$$

$$K_{ij} = \frac{\partial^2 W}{\partial u_i \partial u_j} \quad (6)$$

Where $\mathbf{u}$ denote the particle displacement vector of this bond cell.

3. Consideration of plasticity in SW-DVIB

Ding et al [5] considered the plasticity in DVIB by the following two-body potential Γ, whose first derivative reads

$$\Gamma'(l) = \begin{cases} k_e(l-l_0) & l \le l_y \quad \text{Elastic} \\ k_e(l_y - l_0) + k_p(l - l_y) & l_y \le l \le l_b \quad \text{Plastic} \\ k_e(l-l_0) - (k_e - k_p)(l_{uP} - l_y) & l_y \le l \le l_{uP} \quad \text{Unloading-P} \\ k_e(l_b - l_p^*)\cdot\left(\dfrac{l_f - l}{l_f - l_b}\right) & l_b \le l \le l_f \quad \text{fracturing} \\ k_e(l_b - l_p^*)\cdot\left(\dfrac{l_f - l_{uF}}{l_f - l_b}\right)\cdot\left(\dfrac{l - l_p^*}{l_{uF} - l_p^*}\right) & l_p^* \le l \le l_{uF} \quad \text{Unloading-F} \\ 0 & l \ge l_f \quad \text{Failure} \end{cases} \quad (7)$$

where k_e, k_p are the elastic and plastic stiffness of bond, respectively; l_y is the yield bond length; l_b is the transition bond length from plasticity to fracture; l_f is the ultimate failure bond length; l_p^* is the maximum plastic bond length; l_{uP} is the historic maximum unloading bond length in the plastic stage; l_{uF} is the historic maximum unloading bond

length in the fracture stage. The diagram of Γ' is shown in Fig.2.

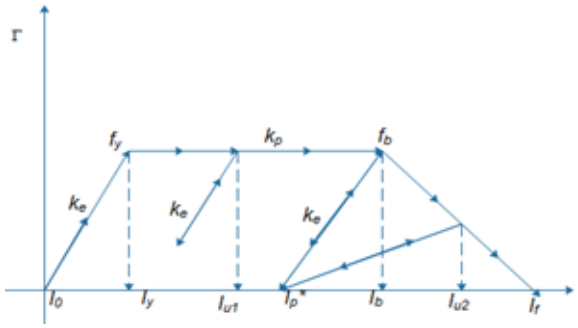

Figure 2: Diagram of the bond force versus bond length of the unified plasticity-fracture bond potential

To embed the plasticity into the SW-DVIB, we take Eq.(7) as the two-body potential ,i.e., $\Phi_2(l)=\Gamma(l)$ and Eq.(3.2) as the three-body potential. Then, by Eqs. (4,5,6), the constitutive relation of a bond cell of:

$$F_i=\frac{\partial W}{\partial u_i}=\frac{1}{2}\sum_I^{N(N-1)}\frac{\partial \Gamma}{\partial l_I}\cdot\frac{\partial l_I}{\partial u_i}+\frac{1}{2}\sum_I^{N(N-1)}\sum_J^{N-2}\frac{\partial \Phi_3}{\partial \theta_{IJ}}\cdot\frac{\partial \theta_{IJ}}{\partial u_i} \quad (8)$$

and the stiffness matrix is

$$K_{ij}=\frac{\partial^2 W}{\partial u_i\partial u_j}=\frac{1}{2}\sum_I^{N(N-1)}\left(\frac{\partial^2\Gamma}{\partial l_I^2}\cdot\frac{\partial l_I}{\partial u_j}\cdot\frac{\partial l_I}{\partial u_i}+\frac{\partial\Gamma}{\partial l_I}\cdot\frac{\partial^2 l_I}{\partial u_i\partial u_j}\right)+\frac{1}{2}\sum_I^{N(N-1)}\sum_J^{N-2}\left(\frac{\partial^2\Phi_3}{\partial\theta_{IJ}^2}\cdot\frac{\partial\theta_{IJ}}{\partial u_j}\cdot\frac{\partial\theta_{IJ}}{\partial u_i}+\frac{\partial\Phi_3}{\partial\theta_{IJ}}\cdot\frac{\partial^2\theta_{IJ}}{\partial u_i\partial u_j}\right) \quad (9)$$

Substituting Eq.(7) and Eq.(3.2) into Eq.(8) and Eq.(9), the specific expression of constitutive relation of elastoplastic SW-DVIB is obtained

$$F_i=\frac{\partial W}{\partial u_i}=\frac{1}{2}\sum_I^{N(N-1)}\Gamma'\cdot\frac{\partial l_I}{\partial u_i}+\frac{1}{2}\sum_I^{N(N-1)}\sum_J^{N-2}\lambda(\theta_{IJ}-\theta_{IJ0})\cdot\frac{\partial\theta_{IJ}}{\partial u_i} \quad (10)$$

$$K_{ij}=\frac{\partial^2 W}{\partial u_i\partial u_j}=\frac{1}{2}\sum_I^{N(N-1)}\left(\Gamma''\cdot\frac{\partial l_I}{\partial u_j}\cdot\frac{\partial l_I}{\partial u_i}+\Gamma'\cdot\frac{\partial^2 l_I}{\partial u_i\partial u_j}\right)+\frac{1}{2}\sum_I^{N(N-1)}\sum_J^{N-2}\left(\lambda\cdot\frac{\partial\theta_{IJ}}{\partial u_j}\cdot\frac{\partial\theta_{IJ}}{\partial u_i}+\lambda(\theta_{IJ}-\theta_{IJ0})\cdot\frac{\partial^2\theta_{IJ}}{\partial u_i\partial u_j}\right) \quad (11)$$

Where the second derivative Γ'' is

$$\Gamma''(l)=\begin{cases}k_e & l\le l_y & \text{Elastic}\\ k_p & l_y\le l\le l_b & \text{Plastic}\\ k_e & l_y\le l\le l_{uP} & \text{Unloading-P}\\ -\dfrac{k_e(l_b-l_p^*)}{l_f-l_b} & l_b\le l\le l_f & \text{fracturing}\\ \dfrac{k_e(l_b-l_p^*)}{l_{uF}-l_p^*}\cdot\dfrac{l_f-l_{uF}}{l_f-l_b} & l_p^*\le l\le l_{uF} & \text{Unloading-F}\\ 0 & l\ge l_f & \text{Failure}\end{cases} \quad (12)$$

As for the other derivatives, e.g. $\partial l/\partial u_i$, $\partial\theta_{IJ}/\partial u_i$, refers to Zhang and Chen [8].

According to Zhang and Chen [8], the bond potential parameters are calibrated as

$$k_e=\frac{2V}{N(N-1)l_0^2}\cdot\frac{3E}{(1-2\nu)}$$
$$\lambda=\frac{V}{N(N-1)(N-2)}\cdot\frac{9E(1-4\nu)}{2(1+\nu)(1-2\nu)} \quad (13)$$

Where V the volume of a unit cell is, E is Young's modulus and ν is the Poisson ratio.

4. Simulation Examples

To show the performance of the presented model, we simulate a uniaxial loading-unloading test reported in the case reported in Chen et al [10]. The geometry and the meshing scheme of the simulated specimen are shown in Fig.3. The restriction boundary at the left side of the plate subjected to the loading-unloading condition is shown in Fig.4. The material parameters provided in fig.4. are: the tangent modulus E= 69 GPa, the plastic tangent modulus Ep= 0.69 GPa, the yield strength σy = 200 MPa, the material density ρ= 2700 kg/m2. To validate the present method, we simulate the plate following the loading-unloading path shown in fig.4. The simulated reaction at the loading point is reported in fig.5, which shows that the present method can simulate the plastic response of material under loading-unloading condition.

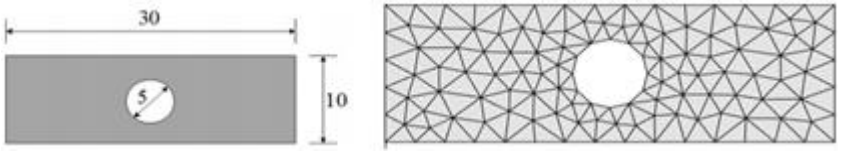

Figure 3: Simulation object and meshing scheme for plastic deformation,(unit: mm).

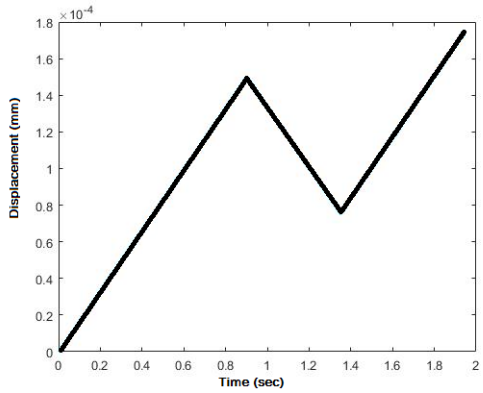

Figure 4: Restriction boundary at the left side of the plate subjected to the loading-unloading condition.

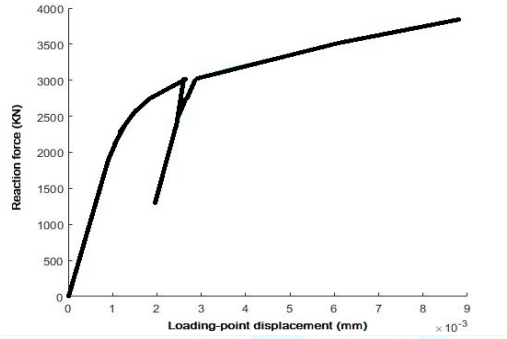

Figure 5: Simulated reaction at the right side of plate

5. Conclusion

By embedding the plasticity into the two-body interaction of SW potential, the SW-DVIB can account for the plastic deformation. Compared with the plastic DVIB, the SW-DVIB can represent the variable Poisson ratios. The simulation result demonstrates that the SW-DVIB can reproduce the loading-unloading plastic behaviors of material. The SW-DVIB is promising approach to simulate the plastic fracture.

References

[1] Xu Y, Chen J, Li H. Finite hyperelastic–plastic constitutive equations for atomistic simulation of dynamic ductile fracture. Int J Plast 2014; 59:15–29.
[2] Zapperi S, Vespignani A, Stanley HE. Plasticity and avalanche behaviour in micro-fracturing phenomena. Nature 1997; 388:658–60.
[3] Seppala ET, Raisanen VI, Alava MJ. Scaling of interfaces in brittle fracture and perfect plasticity. Phy Rev E 2000;61:6312–9.
[4] Picallo CB, Lopez JM, Zapperi S, Alava MJ. From brittle to ductile fracture in disordered materials. Phy Rev Lett 2010;105:155502.
[5] Ding J, Zhang Z, Yang F, Zhao Y, Ge X. Plastic fracture simulation by using discretised virtual internal bond. Engineering Fracture Mechanics 178 (2017) 169–183
[6] Zhang Z. Discretised virtual internal bond model for nonlinear elasticity. International Journal of Solids and Structures 50 (2013) 3618–3625
[7] Zhang Z, Chen YX. Modelling nonlinear elastic solid with correlated lattice bond cell for dynamic fracture simulation. Comput Methods Appl Mech Eng 2014;279:325–47
[8] Zhang Z, Chen Y, Zheng H. A modified Stillinger–Weber potential-based hyperelastic constitutive model for nonlinear elasticity. International Journal of Solids and Structures 51 (2014) 1542–1554.
[9] Stillinger, F. H. and T. A. Weber (1985). "Computer simulation of local order in condensed phases of silicon." Phys. Rev. B 31(8): 5262 - 5271.
[10] Chen H, Lin E, Liu Y. A novel volume-compensated particle method for 2D elasticity and plasticity analysis. Int J Solid Struct 2014; 51:1819-1833.